

Electric transport behaviour of sodium-substituted perovskites  $\text{La}_{1-x}\text{Na}_x\text{MnO}_3$  (for  $x = 0.1$  and  $0.2$ ) and the effect of magnetic fields

This article has been downloaded from IOPscience. Please scroll down to see the full text article.

2008 J. Phys.: Condens. Matter 20 425220

(<http://iopscience.iop.org/0953-8984/20/42/425220>)

View [the table of contents for this issue](#), or go to the [journal homepage](#) for more

Download details:

IP Address: 129.252.86.83

The article was downloaded on 29/05/2010 at 16:00

Please note that [terms and conditions apply](#).

# Electric transport behaviour of sodium-substituted perovskites $\text{La}_{1-x}\text{Na}_x\text{MnO}_3$ (for $x = 0.1$ and $0.2$ ) and the effect of magnetic fields

M P Sharma<sup>1</sup>, Anjali Krishnamurthy<sup>1</sup>, Bipin K Srivastava<sup>1</sup>, S K Jain<sup>2</sup> and A K Nigam<sup>3</sup>

<sup>1</sup> Department of Physics, University of Rajasthan, Jaipur 302004, India

<sup>2</sup> ICFAI Tech University, Jaipur 302022, India

<sup>3</sup> Tata Institute of Fundamental Research, Mumbai 400085, India

E-mail: [mps\\_45@yahoo.com](mailto:mps_45@yahoo.com)

Received 19 May 2008, in final form 29 August 2008

Published 30 September 2008

Online at [stacks.iop.org/JPhysCM/20/425220](http://stacks.iop.org/JPhysCM/20/425220)

## Abstract

Sodium-substituted perovskites  $\text{La}_{0.9}\text{Na}_{0.1}\text{MnO}_3$  and  $\text{La}_{0.8}\text{Na}_{0.2}\text{MnO}_3$ , which crystallize in pseudo-cubic symmetry, and are respectively a disordered and an ordered ferromagnet, have been studied for their electrical behaviour. The two samples show large negative magnetoresistance. The lesser sodium-containing system shows a metal–insulator transition at  $\sim 210$  K, which is well below the temperature where it completely goes to the paramagnetic state. In the higher sodium-containing sample both the magnetic and electrical transitions would fall only above 300 K. In the conducting state in both samples, resistivity has contributions from scattering from grain boundaries, electron–electron scattering and electron–magnon (spin wave) scattering. However, in the insulating (semiconducting) state even the lesser sodium-containing system (in which the insulating state has been observed in the temperature range of study) follows small polaron hopping under an adiabatic approximation and the estimated activation energy values at different fields are also identical to those reported in magnetically ordered perovskites.  $\text{La}_{0.9}\text{Na}_{0.1}\text{MnO}_3$  shows an upturn in resistivity with decreasing temperature at  $\sim 30$  K which is attributed to spin-polarized intergranular tunnelling.

## 1. Introduction

Lanthanum manganites with substitutions at both La and Mn sites have drawn considerable attention as they exhibit interesting phenomena such as colossal negative magnetoresistance, magnetic, structural and metal–insulator phase transition and a charge or polaron ordering, e.g. [1–5].  $\text{LaMnO}_3$  is a Mott insulator and has a canted antiferromagnetic layer structure. As regards the effect of substitutions at the La site, mostly those for divalent cations like  $\text{Ca}^{2+}$ ,  $\text{Sr}^{2+}$ ,  $\text{Ba}^{2+}$  and  $\text{Pb}^{2+}$  have been investigated. Studies have shown that substitution of more than 1/3rd of  $\text{La}^{3+}$  atomic fraction by divalent cations leads to an ordered ferromagnetic state associated with an insulator–metal transition. This is explained in terms of double exchange between  $\text{Mn}^{3+}$  and  $\text{Mn}^{4+}$  [1–3]. We have undertaken a study

on the effect of substitution of monovalent cation  $\text{Na}^+$  for  $\text{La}^{3+}$  in  $\text{LaMnO}_3$ . In this paper we present results on the electrical behaviour of the samples including the effect of the magnetic field. Electrical resistivity has been studied in zero field and in fields up to 9 T and at temperatures down to 5 K. Results have been discussed in the light of literature reports on other substituted perovskites.

## 2. Experimental details and structural characterization

Samples of the compositions  $\text{La}_{0.9}\text{Na}_{0.1}\text{MnO}_3$  and  $\text{La}_{0.8}\text{Na}_{0.2}\text{MnO}_3$  studied here are the same as reported in our earlier paper [6]. The samples were prepared by the sol–gel technique followed by heat treatment at  $900^\circ\text{C}$  in open air atmosphere

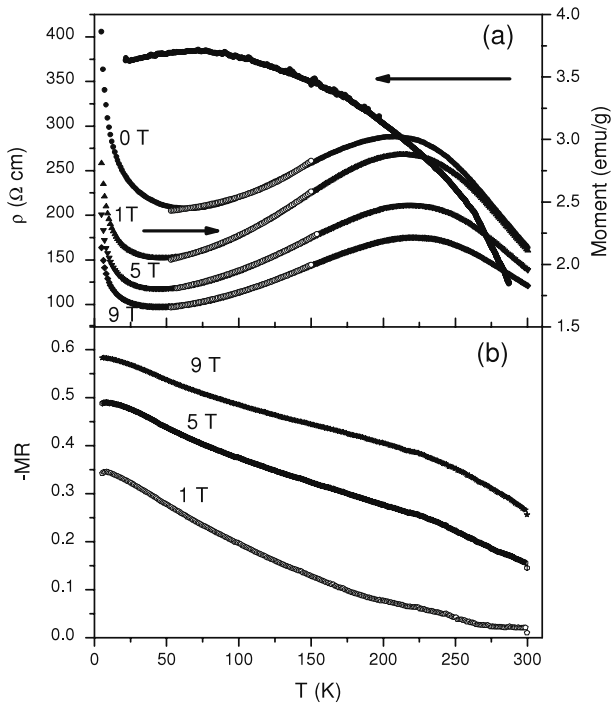


**Figure 1.** (a) Variation of resistivity of LSM10 with temperature under different magnetic fields. Fitting of the function  $\rho = \rho_0 + \rho_2 T^2 + \rho_{4.5} T^{4.5}$  is also shown (by open circles) in the conducting region (variation of magnetization versus temperature in a magnetic field of 504 Oe is also shown). (b) Variation of magnetoresistance of LSM10 with temperature under different magnetic fields.

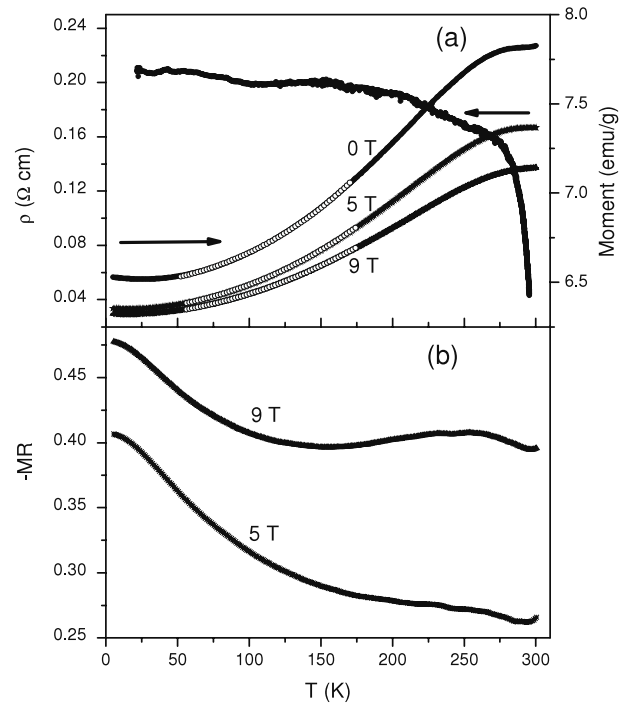


**Figure 2.** (a) Variation of resistivity of LSM20 with temperature under different magnetic fields. Fitting of the function  $\rho = \rho_0 + \rho_2 T^2 + \rho_{4.5} T^{4.5}$  is also shown (by open circles) in the conducting region (variation of magnetization versus temperature in a magnetic field of 100 Oe is also shown). (b) Variation of magnetoresistance of LSM20 with temperature under different magnetic fields.

for 4 d. The two samples, hereafter referred to as LSM10 and LSM20, respectively crystallize in pseudo-cubic symmetry with cell constant  $a \sim 3.8 \text{ \AA}$ . Resistivity measurements have been made on sintered pellets using the four-probe method, in external magnetic fields up to 9 T and at temperatures down to 5 K, on a Quantum Design Physical Property Measurement System (PPMS).

### 3. Results and discussion

#### 3.1. General

Figure 1(a) shows variation of electrical resistivity ( $\rho$ ) with temperature ( $T$ ) for sample LSM10 at magnetic fields of 0, 1, 5 and 9 T (magnetization–temperature ( $M$ – $T$ ) variation is also shown for the purpose of comparison). Magnetoresistance (MR), defined as  $(R_H - R_{0H})/R_{0H}$ , for LSM10 is plotted as a function of temperature in figure 1(b). Figures 2(a) and (b) show plots of the temperature dependence of resistivity ( $\rho$ ) and MR, respectively, for sample LSM20; in figure 2(a) the  $M$ – $T$  variation is also shown for the purpose of comparison.

LSM20 shows a metallic state between 20 and 295 K. The fact that this sample has an ordered FM state below  $\sim 295 \text{ K}$  at which it shows a reasonably sharp PM–FM transition underlines the significance of electron hopping both in electrical conduction and in the manifestation of FM order. In sample LSM10, with lower sodium substitution, the nature of electrical conduction switches over from metallic to

insulating at  $\sim 220 \text{ K}$  whereas the broad transition from the FM state to the PM state seems to become complete only above 300 K. The observed difference between the metal–insulator transition temperature and the Curie temperature has been seen in many other polycrystalline manganites and presumably occurs due to poor connectivity between grains, e.g. [7, 8]. In manganites, the electrical transport behaviour has been found to be strongly dependent on the grain size, grain boundaries and the interconnectivity between them. A model has been proposed based on parallel conduction channels of good and poor conductivity, to explain the electrical transport behaviour in  $\text{La}_{0.7}\text{Ca}_{0.3}\text{MnO}_3$  similar to that observed in the present study [8]. This model can also be conceived in terms of regions of ferromagnetic conducting grains separated by antiferromagnetic insulating grains or regions. In LSM10, the higher resistivity (by 3–4 orders of magnitude than for LSM20) is presumably due to the existence of larger number of AFM grains which result in poor conductivity. Application of a field promotes intergranular tunnelling, thereby decreasing the resistivity [9].

Another observation to be noted is a steep increase in resistivity of LSM10 at a low temperature of  $\sim 30 \text{ K}$ . This could also be explained on the basis of the same model. If two grains have different orientations of their magnetizations, they would have different channels of up and down spins separated by an energy gap. If an electron then tunnels (conserving its spin angular momentum) through the disordered grain boundary

**Table 1.** The best fit parameters obtained from fitting of low temperature resistivity–temperature data in the sample  $\text{La}_{0.9}\text{Na}_{0.1}\text{MnO}_3$ .

Field (T)	$\rho_0$ ( $\Omega$ cm)	$\rho_2$ ( $\Omega$ cm $\text{K}^{-2}$ )	$\rho_{4.5}$ ( $\Omega$ cm $\text{K}^{-4.5}$ )	$\chi^2$
0	200	$1.66 \times 10^{-3}$	$3.76 \times 10^{-9}$	99.313
1	139	$3.65 \times 10^{-3}$	$0.67 \times 10^{-9}$	99.917
5	108	$2.93 \times 10^{-3}$	$0.09 \times 10^{-9}$	99.957
9	89	$2.31 \times 10^{-3}$	$0.36 \times 10^{-9}$	99.926

**Table 2.** The best fit parameters obtained from fitting of low temperature resistivity–temperature data in the sample  $\text{La}_{0.8}\text{Na}_{0.2}\text{MnO}_3$ .

Field (T)	$\rho_0$ ( $\Omega$ cm)	$\rho_2$ ( $\Omega$ cm $\text{K}^{-2}$ )	$\rho_{4.5}$ ( $\Omega$ cm $\text{K}^{-4.5}$ )	$\chi^2$
0	0.0504	$2.35 \times 10^{-6}$	$6.65 \times 10^{-13}$	99.988
5	0.0312	$1.95 \times 10^{-6}$	$1.94 \times 10^{-13}$	99.998
9	0.0276	$1.56 \times 10^{-6}$	$0.14 \times 10^{-13}$	99.998

region, it will experience an energy barrier [10]. This would lead to an increase in resistance at low temperature due to an activated or variable range hopping process in the grain boundary region if the spin-polarized tunnelling remains the dominant electron transport mechanism.

The magnetoresistance (MR) is observed to be negative and large. It is to be noted that the magnetoresistance at 5 T field is about 50% at 20 K in both samples. Further, in LSM10, where a clear metal to insulator (M–I) transition shows up (at  $\sim 200$  K in zero field), the transition point shifts to higher temperature with increasing field. It occurs due to an increase in hopping conductivity (due to double exchange) resulting from increased ferromagnetic alignment of Mn spins.

### 3.2. Resistivity–temperature data in conducting region

To understand the scattering mechanisms contributing to resistivity, we have fitted the  $\rho$ – $T$  curves with a polynomial function. Now, in literature reports, e.g. [1, 11, 12],  $\rho$ – $T$  curves have been analysed in terms of the following functions: (i)  $\rho = \rho_0 + \rho_2 T^2$ , (ii)  $\rho = \rho_0 + \rho_{2.5} T^{2.5}$  and (iii)  $\rho = \rho_0 + \rho_2 T^2 + \rho_{4.5} T^{4.5}$  where  $\rho_0$  represents contributions to resistivity from grain boundaries,  $\rho_2$  corresponds to contributions from electron–electron scattering and  $\rho_{4.5}$  corresponds to scattering with spin waves (magnons). In the two samples studied here, best fittings could be obtained with the function  $\rho = \rho_0 + \rho_2 T^2 + \rho_{4.5} T^{4.5}$ . The fittings are shown in figures 1(a) and 2(a). Tables 1 and 2 give the obtained values of  $\rho_0$ ,  $\rho_2$  and  $\rho_{4.5}$  for the two samples at different fields. The orders of magnitude of the obtained values of  $\rho_2$  and  $\rho_{4.5}$  for sample LSM20 agree with the literature reported values (cf, e.g., [11]). For LSM10 the values of the temperature-independent resistance and also of the two coefficients are higher by several orders of magnitude.

For both the samples, the three coefficients show a general reduction with increasing magnetic field. This is in accordance with observations reported in the literature (e.g. [12]). An increasing field enlarges the magnetic domain which causes  $\rho_0$  to decrease. Reduction in  $\rho_2$  and  $\rho_{4.5}$  with increasing field is due to decreasing spin fluctuations.

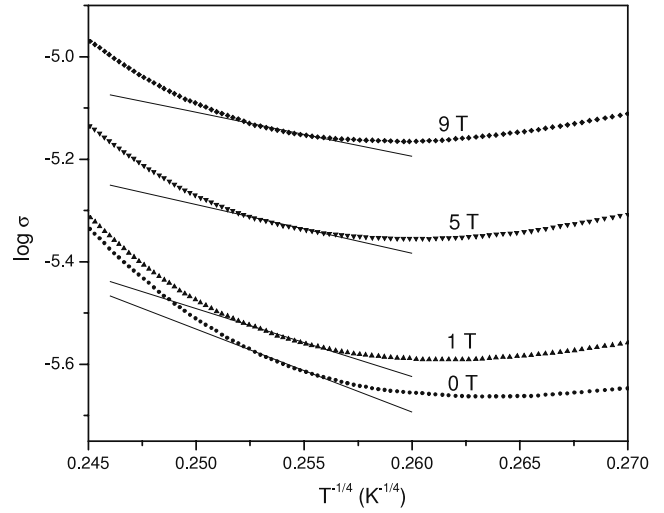


**Figure 3.** Plot of  $\log \sigma$  versus  $T^{-1/4}$  for LSM10 in insulating region under different magnetic fields. Solid line shows the fitted function.

**Table 3.** Values of  $T_0$ , density of state at Fermi energies and activation energies (cf text) obtained from fitting of high temperature resistivity–temperature data of the sample  $\text{La}_{0.9}\text{Na}_{0.1}\text{MnO}_3$ .

Field (T)	$T_0$ (K)	$N(E_F)$ ( $\text{eV}^{-1} \text{cm}^{-3}$ )	Activation energy (meV)
0	68 925	$29.4489 \times 10^{21}$	87.4
1	30 866	$65.7606 \times 10^{21}$	85.5
5	8 283	$245.0521 \times 10^{21}$	76.5
9	5 421	$374.4266 \times 10^{21}$	70.2

### 3.3. Resistivity–temperature data of LSM10 in the insulating region

The variation of resistivity (conductivity) in the insulating region just above the M–I transition temperature  $T_p$  but below  $\theta_D/2$  (i.e.  $T_p < T < \theta_D/2$ ) is explained by the variable range hopping (VRH) model (e.g. [11, 12]):

$$\sigma = \sigma_0 \exp(-T_0/T)^{1/4}.$$

We have fitted our data just above  $T_p$  in the VRH model. Figure 3 shows the fitting. The obtained values of  $T_0$  are given in table 3. Using these  $T_0$  values, the density of states at the Fermi level,  $N(E_F)$ , have been estimated using the relation  $T_0 = 16\alpha^3/k_B N(E_F)$  and assuming  $\alpha$  to be a constant at  $2.22 \text{ nm}^{-1}$  [11, 13]. Estimated values of  $N(E_F)$  are also given in table 3. The estimated values of  $N(E_F)$  are a few orders of magnitude higher than those in oxide semiconductors. This is suggestive of the applicability of the small polaron hopping mechanism under adiabatic approximation in the higher temperature regions, namely  $T > \theta_D/2$  [12].

Accordingly, we have fitted our resistivity data in the higher temperature limit ( $T > \theta_D/2$ ) in the small polaron hopping model in the adiabatic approximation. In this model the resistivity variation with temperature goes as

$$\rho/T = \rho_\alpha \exp(E_P/k_B T)$$

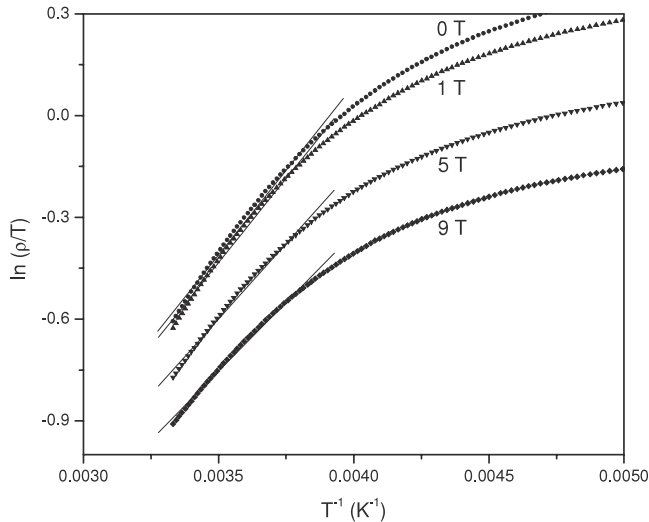


**Figure 4.** Variation of  $\ln(\rho/T)$  with  $T^{-1}$  for LSM10 in insulating region under different magnetic fields. The solid line shows fitting to the equation  $\rho/T = \rho_\alpha \exp(E_P/k_B T)$ .

where  $\rho_\alpha$ , the residual resistivity, is a function of electronic charge, phonon frequency, number density of charge carriers and average inter-site spacing,  $E_P$  is the activation energy and  $k_B$  is Boltzmann's constant. Figure 4 shows the fitting. Estimated activation energies at different fields are given in table 3. The values are of the same order as reported for other manganite perovskites (e.g. [11]). This implies that the insulating (semiconducting) state in the lower sodium-containing sample LSM10 is identical to that in magnetically well-ordered (in FM state) perovskite systems. Also as expected  $E_P$  decreases with increasing field, which may be due to decreasing charge localization with increasing magnetic field.

#### 4. Conclusion

The variation of electrical resistivity with temperature for the 20 at.% sodium-substituted ordered ferromagnet LSM20, shows metallic behaviour as is also reported for divalent-cation-substituted long range ordered FM perovskites. Also the magnitude of the estimated electron–electron and spin wave magnetic scattering contributions for LSM20 are comparable with reported values for divalent-cation-substituted long range ordered FM perovskites. The 10 at.% sodium-substituted system LSM10, which is a disordered FM, undergoes an M–I transition at a temperature well below where it completes

its transition from the FM to PM state and the magnitudes of the estimated electron–electron and spin wave magnetic scattering contributions are higher by orders of magnitude. However, as regards the semiconducting (insulating) region, the lower sodium-containing sample LSM10 (in whose case the semiconducting (insulating) state has been observed in the temperature range of study) follows, as do magnetically ordered perovskites, small polaron hopping under the adiabatic approximation and the estimated activation energy values at different fields are also identical to those reported in magnetically ordered perovskites. Both the samples exhibit rather large magnetoresistance. The magnetically disordered system LSM10 shows an upturn in resistivity with decreasing temperature at  $\sim 30$  K. This behaviour seems to be caused by the spin-polarized intergranular tunnelling.

#### Acknowledgments

Thanks are due to Sri Devendra Buddhikot for the resistivity measurements. This work has been done under a UGC funded project and their financial assistance is gratefully acknowledged. One of us (MPS) thanks CSIR for the award of a research fellowship.

#### References

- [1] Schiffer P, Ramire A P, Bao W and Cheong S W 1995 *Phys. Rev. Lett.* **75** 3336
- [2] Gayathri N, Raychaudhuri A K, Tiwari S K, Gundakaram R, Arulraj A and Rao C N R 1997 *Phys. Rev. B* **56** 1345
- [3] Zener C 1951 *Phys. Rev.* **83** 440
- [4] Itoh M, Shimura T, Yu J-D, Hayashi T and Inaguma Y 1995 *Phys. Rev. B* **52** 12522
- [5] Weast R C 1971–1972 *CRC Handbook of Chemistry and Physics* 52nd edn (Boca Raton, FL: CRC Press)
- [6] Sharma M P, Jain S K, Krishnamurthy A and Srivastava B K 2008 *Ind. J. Pure Appl. Phys.* **46** 325
- [7] Biswas A and Das I 2007 *J. Appl. Phys.* **102** 064303
- [8] Andres A de, Garcia-Hernandez M and Merinez J L 1999 *Phys. Rev. B* **60** 7328
- [9] Raychaudhuri P, Sheshadri K, Taneja P, Bandopadhyay S, Ayuub P, Nigam A K and Pinto R 1999 *Phys. Rev. B* **59** 13919
- [10] Raychaudhuri P, Taneja P, Nigam A K, Ayuub P, Pinto R and Patade A 1999 *Physica B* **259–261** 812
- [11] Banerjee A, Pal S and Chaudhari B K 2001 *J. Chem. Phys.* **115** 1550
- [12] Padmavathi K, Venkataiah G and Reddy P V 2007 *J. Magn. Mater.* **309** 237
- [13] Viret M, Rannoand L and Coey J M D 1997 *Phys. Rev. B* **55** 8067